Construction and Building Materials 145 (2017) 226–235

Contents lists available at ScienceDirect

Construction and Building Materials

journal homepage: www.elsevier.com/locate/conbuildmat

Timber moment connections using glued-in basalt FRP rods

Caoimhe O'Neill [a,*], Daniel McPolin [a], Su E. Taylor [a], Annette M. Harte [b], Conan O'Ceallaigh [b], Karol S. Sikora [b]

[a] Civil Engineering Research Centre, School of Natural and Built Environment, Queen's University Belfast, BT9 5AG, UK
[b] College of Engineering and Informatics, National University of Ireland Galway, Galway, Ireland

HIGHLIGHTS

- Glued-in rods as moment connections in partial portal frames was investigated.
- Design was based on failure of the timber surrounding the glued-in rod connection.
- Additional rods do not significantly impact the strength of the frame.

ARTICLE INFO

Article history:
Received 10 June 2016
Received in revised form 15 March 2017
Accepted 31 March 2017
Available online 9 April 2017

Keywords:
Timber
Glued-in rods
Bonded-in rods
Basalt fibre reinforced polymer
BFRP
Composites
Portal frames

ABSTRACT

Glued-in rods offer an alternative method for creating structural timber connections however despite decades of research they have had limited implementation. The behaviour of glued-in rod connections in a framed structure was investigated. Nine partial frames were constructed of box sections connected with 12 mm diameter BFRP rods. A theoretical design approach was developed based on the optimum observed behaviour, where failure was located in the connection. For specimens with two embedded rods the theory predicted strength within 16% error of the experimental results. For specimens with two rods but gave an over-prediction of strength where three rods were used.

1. Introduction

Glued-in rods (GiR) have a wide range of uses in both new build and restoration projects where they offer an alternative to traditional connection and reinforcement methods. Successful renovation using glued-in rods has been carried out in roof and floor beams in buildings subject to decay [1,2]. In new build, five areas were identified where GiR may be used for connections: frame corner, beam-post connection, beam-beam joint, supports and hinged joints [3]. It is the frame corner application that is examined in this study. Currently most timber moment connections, such as in a timber portal frame structure, are created typically either using a steel bracket spliced with the timber elements or through the use of plywood sheathing, splicing both timber elements. In both scenarios a haunch is normally used. For connections made with plywood sheathing, the haunch is normally much larger in proportion compared to the equivalent steel. GiR can distribute stresses very effectively, combining the benefits of high strength materials and effective material interfaces thus offering the potential for a smaller and neater connection.

Since the late 1980s there have been many research projects commissioned on the use of GiR in timber construction e.g. GIROD and LICONS [4,5]. In spite of this, no universal standard exists for their design. There had been an informative annex in the pre-standard PrBS ENV 1995-2:1997 which provided limited coverage of the design of GiR using steel bars however this document was replaced by BS EN 1995-2:2004 and no guidance is included in this current document.

Previous new build that has used the GiR connection method has used steel rods embedded into large glulam elements. In this experimental programme, the timber box sections used are constructed primarily of C16 Irish grown Sitka spruce (Pieca sitchensis) solid timber flanges and orientated strand board (OSB) or plywood webs. The rods used are basalt fibre reinforced polymer (BFRP). Despite its significant cost effectiveness compared to

* Corresponding author.
E-mail addresses: coneill86@qub.ac.uk (C. O'Neill), d.mcpolin@qub.ac.uk (D. McPolin), s.e.taylor@qub.ac.uk (S.E. Taylor), annette.harte@nuigalway.ie (A.M. Harte), conan.oceallaigh@nuigalway.ie (C. O'Ceallaigh), karol.sikora@nuigalway.ie (K.S. Sikora).

http://dx.doi.org/10.1016/j.conbuildmat.2017.03.241
0950-0618/

Carbon FRP and its greater tensile strength compared to Glass FRP, BFRP has only been investigated in a very limited manner for use in glued-in technology [6]. BFRP has a modulus of elasticity closer to timber than the more commonly used steel and has a significantly better weight to strength ratio. These advantages make glued-in BFRP rods an attractive connection method where a lightweight, durable and sustainable building solution is required. In order to investigate the behaviour of such a connection in service, nine partial portal frames (frame corners) were built and tested to failure, as summarised below.

The overall aim of this study focuses on the end use of BFRP GiR in large scale structures which require moment resisting connections such as portal frames buildings. The use of GiR connections in solid C16 Sitka spruce is investigated. Following assessment of the performance of individual glued-in BFRP rods in a simplified pull-out test, the experiment presented in this paper further investigates how GiR perform under a combined axial force and bending moment. Partial portal frames were built to scale and GiR used as the connectors between the post and beam. Load testing was carried out to determine the performance of the GiR as moment resisting connections.

The strength of the system, the strains and the deflections were measured as a method of assessing the performance of the GiR moment connections. The behaviour of the connections with varying number of rods in box sections of varying strength were studied.

2. Preliminary investigations

2.1. Background

Embedded length, l_b, is one of the most influential variables on the strength of GiR. A preliminary study was performed to assess how embedded length affected the pull-out strength of glued-in BFRP rods in solid C16 Irish Sitka spruce (Picea sitchensis) [7]. Pull-out strength can be used as a measure of the strength of a GiR. The pull-out test system used was a pull-bending set-up as illustrated in Fig. 1. The pull-bending system allows bending strength of the GiR connection to be evaluated by removing the timber in the section being loaded so that the only resistance is from the BFRP bars glued-in to the timber.

The C16 classification indicates that, at a moisture content of 12%, the timber has a 5th percentile bending strength of 16 N/mm^2 and a mean density of 370 kg/m^3 as per BS EN 338:2009 [8]. These strengths were confirmed by material testing at a moisture content of 12%. Bending strength was validated with the standard test method presented in BS EN 408:2010 [9] and was found to be 16.9 N/mm^2. Density was calculated based on measurements of dimensions and weight and was verified using a handheld timber grader. Density was found to be 381 kg/m^3.

The manufacturer's specification provided with the 12 mm diameter BFRP rods reported tensile strength to be 1200 N/mm^2 and modulus of elasticity to be 50 kN/mm^2. These values were determined under a loading rate of 1 kN/s [10].

All specimens had a 2 mm glueline thickness around each embedded rod. The two-component epoxy adhesive used for the GiR had gap-filling capabilities which ensured a good bond along the entire length of rod by filling the void between the rod and the timber. This helps to achieve good adhesion to both the rod material and the timber and higher shear strength and stiffness in the connection than that of the timber being used. The adhesive is thixotropic (it only flows under shear) so is ideal for applications such as overhead beam repair and jointing overhead. The epoxy used had a bond strength of 6–10 N/mm^2 dependant on the adherends used and preparation of the bonding surfaces. The adhesive had a compressive strength greater than 60 N/mm^2 and tensile strength of 38 N/mm^2 [11].

2.2. Preliminary results

Specimens were tested to structural failure. Pull-out strength was measured via the load cell on the testing apparatus and verified by a strain gauge on the BFRP rod at mid-span. As anticipated, and shown in Fig. 2, an increase in pull-out strength was observed with an increase in embedded length. Between the shortest embedded length of $6.6d_r$ (80 mm) and the longest length of $50d_r$ (600 mm) the pull-out strength increased by a factor of 2.13. This was as expected since the larger interface area with each increase in embedded length provides additional resistance to the applied loading.

The German National Annex to Eurocode 5 (DIN 1052:2008 [12]), presented in Eq. (1) provides a consistent prediction of the pull-out strength, P_u, of a GiR, illustrated in Fig. 2, which is typically 10kN lower than the measured load. This prediction is used in Section 4 in the calculation of the strength of the partial portal frame corners.

$$P_u = \pi \cdot d \cdot l_b \cdot f_{k1,d} \quad (1)$$

where

d = nominal diameter of the rod (mm)
l_b = embedded length of rod (mm)
$f_{k1,d}$ = design value of the bondline strength (N/mm^2)

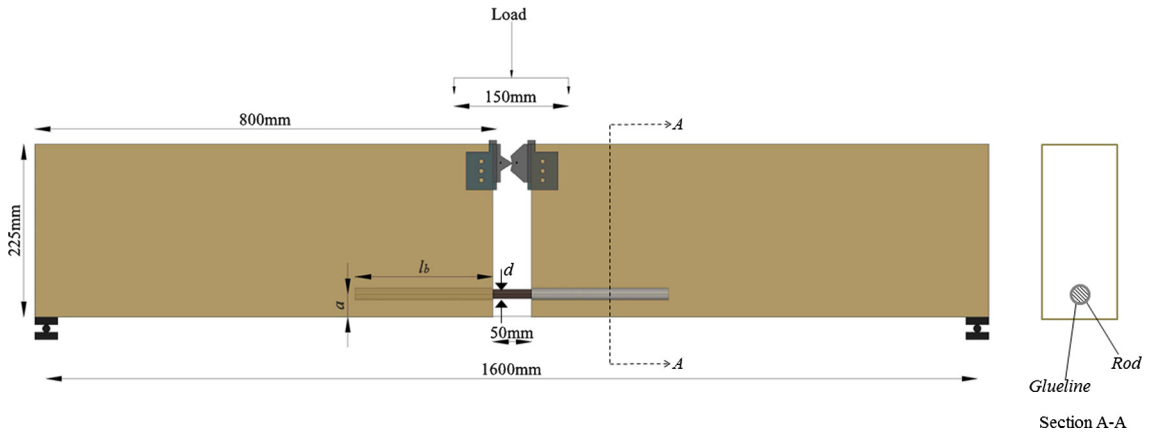

Fig. 1. Pull-bending pull-out test set-up.

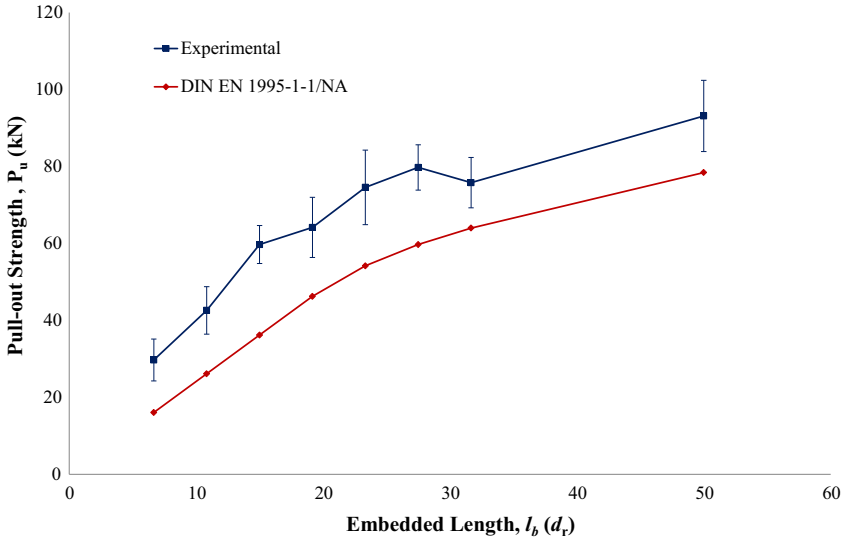

Fig. 2. Pull-bending strength with increasing embedded length.

The design value of the bondline strength, $f_{k1,d}$, is found using Eq. (2):

$$f_{k1,d} = 4.0\ \text{N/mm}^2 \quad \textit{for}\ l_b \leq 250\ \text{mm} \tag{2}$$

$$f_{k1,d} = 5.25 - 0.005 \cdot l_b \quad \text{for}\ 250 < l_b \leqslant 500\ \text{mm}$$

$$f_{k1,d} = 3.5 - 0.0015 \cdot l_b \quad \text{for}\ 500 < l_b \leqslant 1000\ \text{mm}$$

Splitting was observed in all embedded lengths including those of optimum embedded length. In these specimens failure strength was significantly lower than in specimens where no splitting was observed. In an attempt to alleviate this problem, a set of specimens were tested where embedded length remained at $23.3d_r$ (280 mm) but edge distance increased in steps of one bar diameter. It was found that by increasing the edge distance by even a small amount instances of splitting could be reduced or eliminated, thus allowing specimens to reach their full potential strength. The optimum edge distance was identified as $a = 3.5d_r$ (42 mm).

3. Design of moment connection with glued-in rods (GiR)

Within this section GiR will be used to design and create moment resistant connections which would typically appear in portal frame connections. The theoretical capacity of such connections will be determined followed by presentation of the outcome of experimental investigation on partial portal frames of the same size.

3.1. Development of theory

Design of a GiR connection may be considered similarly to the design of a reinforced section. The tested specimens in which the failure mode was where the GiR connection failed were considered to be the optimum failure mode in this study. Thus, the theoretical strain profiles were determined using the GiR at ultimate limit state (ULS). With the GiR governing ULS it was determined theoretically that the stresses in the timber were below the strength of the timber (for a 3 rod system this stress was determined to be 0.13 N/mm^2 and for a 2 rod system it would be less). Consequently the strain and stress profiles in Fig. 3 were developed assuming linear behaviour of the timber [13–15]. The theory assumes also that no bending resistance is provided by the web material to the applied loading. The theory was developed as per the four steps laid out below:

Step 1: Determine dimensions of rod equivalent to timber:
Calculate equivalent timber section
Modular ratio, α_E

$$\alpha_E = \frac{E_{rod}}{E_{timber}} \tag{3}$$

Area of one rod, A_r

$$A_r = \frac{\pi d_r^2}{4} \tag{4}$$

Equivalent area of one rod, A_r'

$$A_r' = \alpha_E A_r \tag{5}$$

Equivalent breadth of one rod, b_r'

$$b_r' = \frac{A_r\prime}{d_r} \tag{6}$$

Step 2: Locate position of neutral axis from top fibre, x, using parallel axis theorem

$$(A_t + nA_r')x = A_t x_t + nA_r' x_r \tag{7}$$

$$x = \frac{A_t x_t + nA_r' x_r}{(A_t + nA_r')} \tag{8}$$

where
A_t = Area of timber
A_r' = Equivalent area of one rod
x = Position of neutral axis from top fibre
x_t = Distance from top fibre to neutral axis of timber element
x_r = Distance from top fibre to neutral axis of rod
n = Number of GiRs

Step 3: Calculate the stresses and strains present in both timber and rod
Stress in one rod, σ_r

$$\sigma_r = \frac{F}{A_r} \tag{9}$$

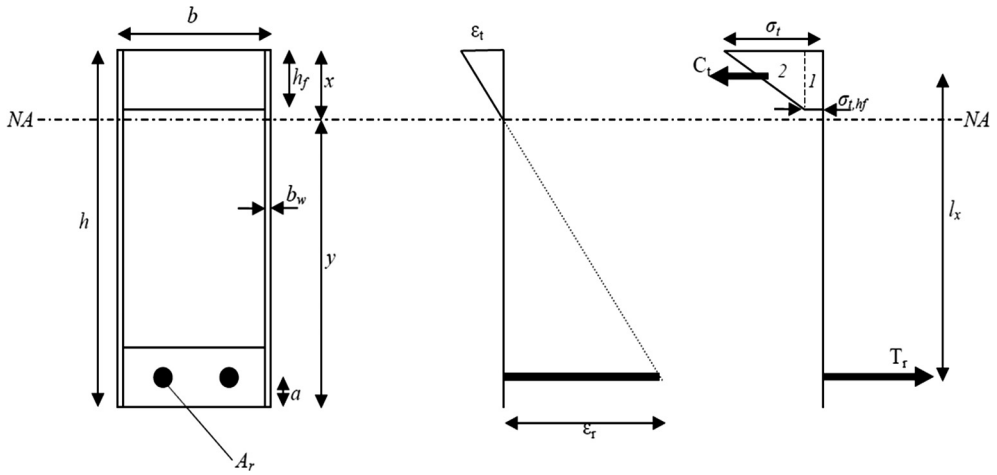

Fig. 3. Stress block in the elastic equilibrium state.

Table 1
Worked example of moment strength calculation.

Moment strength of specimen with two embedded rods		
Materials		
Modulus of elasticity of timber, E_t	9500	N/mm^2
Modulus of elasticity of BFRP rod, E_r	54,000	N/mm^2
Pull-out strength per rod, P_u	40,640	N
Geometric properties of specimen		
Breadth of box section, b	200	mm
Height of box section, h	600	mm
Flange height, h_f	75	mm
Effective height of the section, h_{eff}	562.5	mm
Rod diameter, d	12	mm
Number of rods, n	2	
End distance, a	37.5	mm
Step 1: Determine dimensions of rod equivalent to timber		
Modular ratio, α_E	5.7	
Area of one rod, A_r	113.1	mm^2
Equivalent area of one rod, A'_r	42.9	mm^2
Equivalent breadth of one rod, b'_r	53.6	mm
Locate position of neutral axis from top fibre, x		
x=	78.5	mm
Stress and strain in GiR		
Stress in one rod, σ_r	359.3	N/mm^2
Strain in rod, ε_r	6.7E−03	
Stress and strain in top flange		
Strain at top fibre, ε_t	1.1E−03	
Stress in top fibre, σ_t	10.2	N/mm^2
Strain at bottom of flange, $\varepsilon_{t,hf}$	4.8E−05	
Stress at bottom of flange, $\sigma_{t,hf}$	0.45	N/mm^2
Moment capacity of section, M_t		
C_1	6806.6	N
l_1	525	mm
C_2	73465.8	N
l_2	537.5	mm
M_t	43061359	Nmm
M_t	43.1	kNm

Strain in rod, ε_r

$$\varepsilon_r = \frac{\sigma_r}{E_r} \tag{10}$$

Strain at top fibre, ε_t

$$\frac{\varepsilon_t}{x} = \frac{\varepsilon_r}{y} \tag{11}$$

Stress in top fibre, σ_t

$$\sigma_t = \varepsilon_t E_t \tag{12}$$

At bottom of flange, $\varepsilon_{t,hf}$

$$\frac{\varepsilon_t}{x} = \frac{\varepsilon_{t,hf}}{x - h_f} \tag{13}$$

Stress at bottom of flange, $\sigma_{t,hf}$

$$\sigma_{t,hf} = \varepsilon_{t,hf} E_t \tag{14}$$

Step 4: Calculate the Moment capacity of section, M_t

$$M_t = \sum C_t \cdot l_x \tag{15}$$

3.2. Example of moment strength calculation

The prediction outlined in the worked example in Table 1 below is for a specimen with plywood webs and two embedded rods. It is assumed that plane sections remain plane and that the stress distribution follows the profile in Fig. 3.

Thus it has been shown that for the specimen described above the moment capacity of the assembly has been predicted to be 43.1kNm. Following this development of predicted capacities, partial portal frames were manufactured to determine their actual capacity.

4. Laboratory testing of partial portal frames

4.1. Specimen details and fabrication

Partial portal frames were assembled from box beam and post elements that were 600 mm × 249 mm in overall cross section. The frame corners had a 5° pitch and were constructed as per Fig. 4.

The flange material in all specimens was C16 Irish grown Sitka spruce (Picea sitchensis) solid timber with sawn dimensions of 225 mm × 75 mm, the same material and dimensions as were used in the preliminary tests. The web sheeting material used to create the box was oriented strand board (OSB) manufactured from Irish grown Sitka Spruce (OSB/3 to BS EN 300:2006) or imported Plywood manufactured from Latvian Birch (Betula) of Grade III (BS EN 636:2012). Both OSB and Ply had a thickness of 12 mm. Table 2 provides the details of which materials were used for each specimen set. Web stiffeners in the beam were located above the

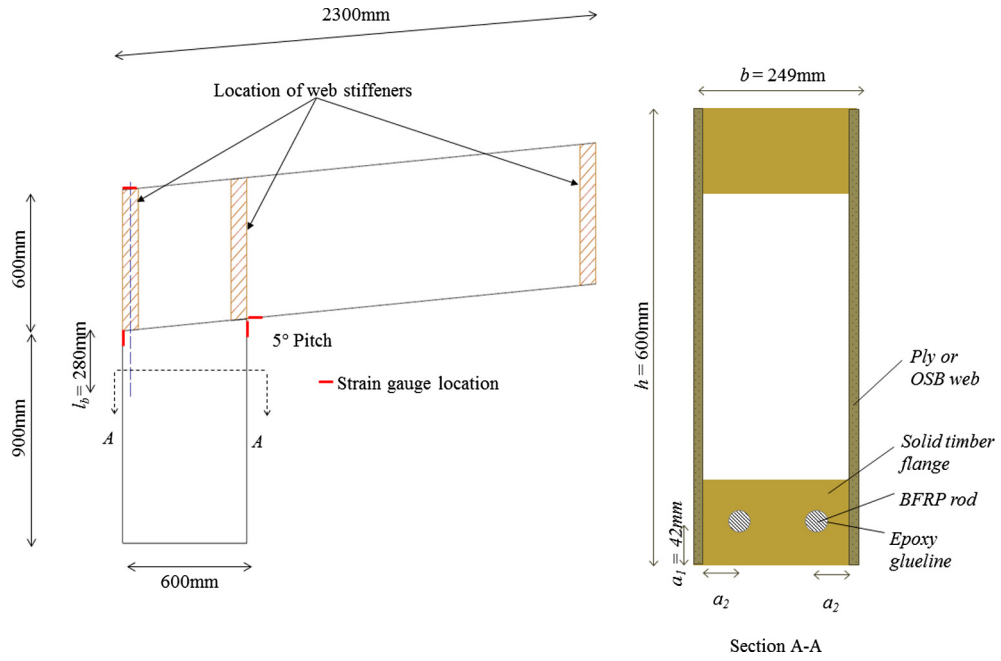

Fig. 4. Frame corner dimensions.

Table 2
Specimen specification.

Set ID	Flange Material	Web Material	No. Rods	No. specimens
OFC_3	C16 Solid timber	OSB/3	3	3
PFC_3	C16 Solid timber	Ply Grade III	3	3
PFC_2	C16 Solid timber	Ply Grade III	2	3

post flanges with the purpose of providing additional anchorage for the GiR. Web stiffeners have the added advantage of preventing buckling of the web.

Holes were drilled vertically through the back end of the beam (through the web stiffener) and into the post using a template to guide the auger, 12 mm diameter Basalt fibre reinforced polymer (BFRP) rods were embedded in the specimens in the configurations detailed in Table 2. The diameter of each rod (12 mm), embedded length (280 mm) and glueline thickness around each rod (2 mm) remained constant throughout this experiment. Information regarding the rod and adhesives used can be found in Section 2.1.

Each specimen set was given an identifier (Set ID) based on web material and number of embedded rods, for instance OFC_3 was an OSB Frame Corner with 3 embedded rods.

Based on the findings of previous research carried out by the authors and summarised in Section 2, an embedded length of $23.3d_r$ (280 mm) was identified as an optimum [7], providing adequate resistance to normal loading conditions expected in service class 1 [16]. Thus the embedded length was set at $l_b = 23.3d_r$ (280 mm) for all specimens in this experiment. Edge distance was chosen based on pull-out testing summarised in the earlier section and set at $a_1 = 3.5d_r$ (42 mm). Edge distance, a_2, was chosen based on the number of rods being used with spacing between each such that rods failed individually rather than as a group. Fig. 5 details the positioning of rods in each set with dimensions given in terms of rod diameter, d_r. Note that the position of rod is given from the outer edge of the flange rather than the outer edge of the web material. An additional web stiffener was inserted at the end of the beam to locate and anchor the BFRP rods in position.

4.2. Test setup

Specimens were tested in a UKCAS calibrated 600 kN hydraulic Dartec actuator as shown in Fig. 6. The specimens were tested to a proof load of 5 kN applied load (equivalent 8.5 kNm moment) before being tested to ultimate failure. The 5 kN proof load corresponds to 40% of the predicted failure load of the weakest specimens, it remained constant throughout the testing to provide a point of reference across all specimens. Loading was increased in 0.5 kN increments in all cases. This generated an equivalent moment increase of 0.85 kNm at each increment.

Readings of strain and deflection were taken at each load increment. As per Fig. 7, deflection was measured at the tip under the load point, along the top face at the back end of the specimen and near to the pivot point. Slip at each side of the post was also recorded as well as rotation about the top left-hand corner. Strain was measured using electric resistance strain (ERS) gauges mounted on the timber surface at the back face close to the beam-post interface.

Specimens were held in place in the testing rig with supports which were bolted to the strong floor under the testing machine and held together with straps. This was representative of a fully fixed support and its effectiveness was assessed in terms of lateral movement using the instrumentation described above.

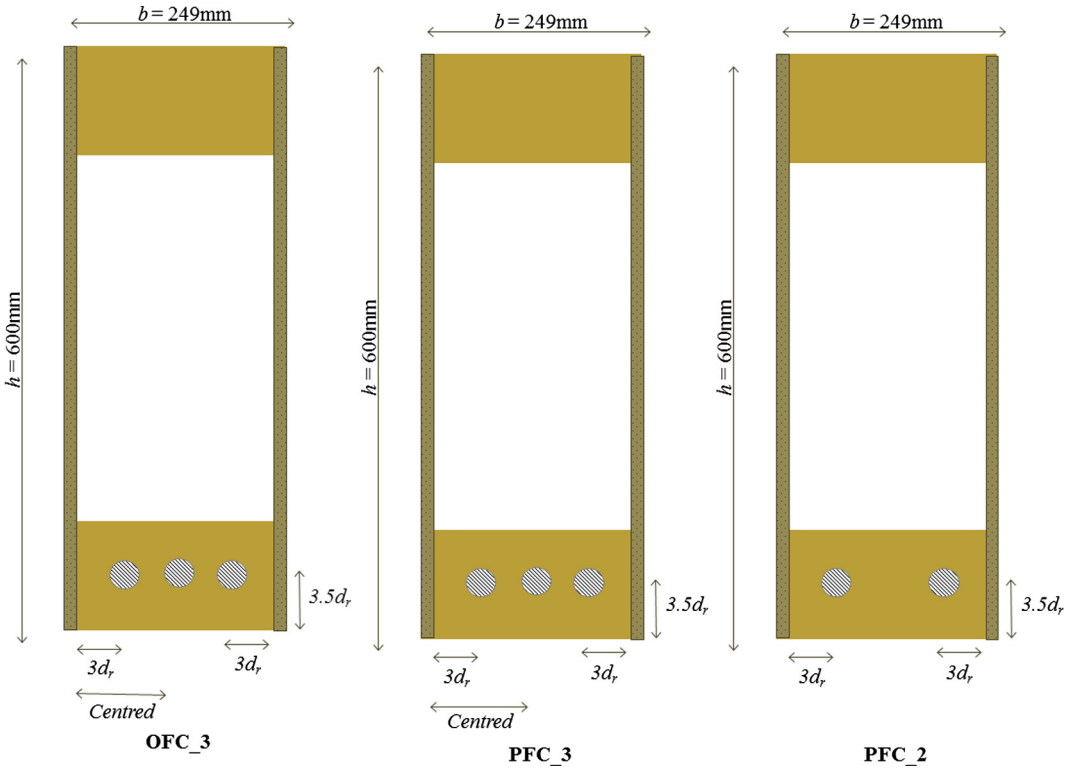

Fig. 5. Hole positions for each GiR (Not to scale).

Fig. 6. Photograph of test set-up in laboratory.

Failure was defined as the point at which the specimen could resist no further increase in load. The structural failure mode was recorded for each specimen, it should be noted that failure was most likely to be serviceability defined with large deflections, however the tests were continued to achieve structural failure where possible for full understanding of the connection behaviour.

4.3. Experimental results

Overall, specimens in the PFC_2 set performed better than the other sets in terms of deflection, failure mode and ultimate strength. However large deflections in all specimens mean that specimens would not be acceptable in terms of serviceability limits. This would require consideration at the design stage to ensure an adequate serviceability performance is achieved. Strength could also be enhanced through the use of a haunch and an additional rod to the front of the post to distribute compression loading more efficiently both of which would aid moment transfer and increase stiffness of the sections.

4.3.1. Deflection

Lateral movement of the post was monitored to allow the contribution from lateral rotation to be removed from the vertical deflection at the tip. An average horizontal movement of 7.6 mm equated to a vertical movement of 14.4 mm at tip. In a full-scale application greater movement would be expected due to the longer length however greater movement is not likely to influence the performance of the moment connection itself. The expected deflection at the end of the cantilever as a result of the beam flexure was also calculated for each specimen. It was found that beam bending would result in an average of 4.2 mm vertical movement downwards.

The results presented in Fig. 8 show deflection as a result of the rotation of the connection system under the applied loading. It can be observed that deflection at the tip increased in an almost linear fashion to ultimate failure. Most linearity was observed in the specimens with Plywood webs with two embedded rods (PFC_2) indicating that this configuration produced a stiffer connection with most effective load transfer.

Deflections were compared at a deflection limit for a cantilever of span/180. This is a typical vertical deflection limit for a cantilever and provided a reference point for all specimens. For the dimensions of the test set-up used this gives a deflection limit of approximately 9.4 mm. At this limit the optimum performance was seen in the PFC_2 set where ultimate strength reached almost 10 kNm. For the other sets a lower strength was reached at the deflection limit. In practice, in order to increase stiffness of the section a minimum of one additional GiR would be embedded in the front face of the post to aid moment transfer. This was not included in the experimental study presented since it was desired that a failure in the back connection should occur and the behaviour of the

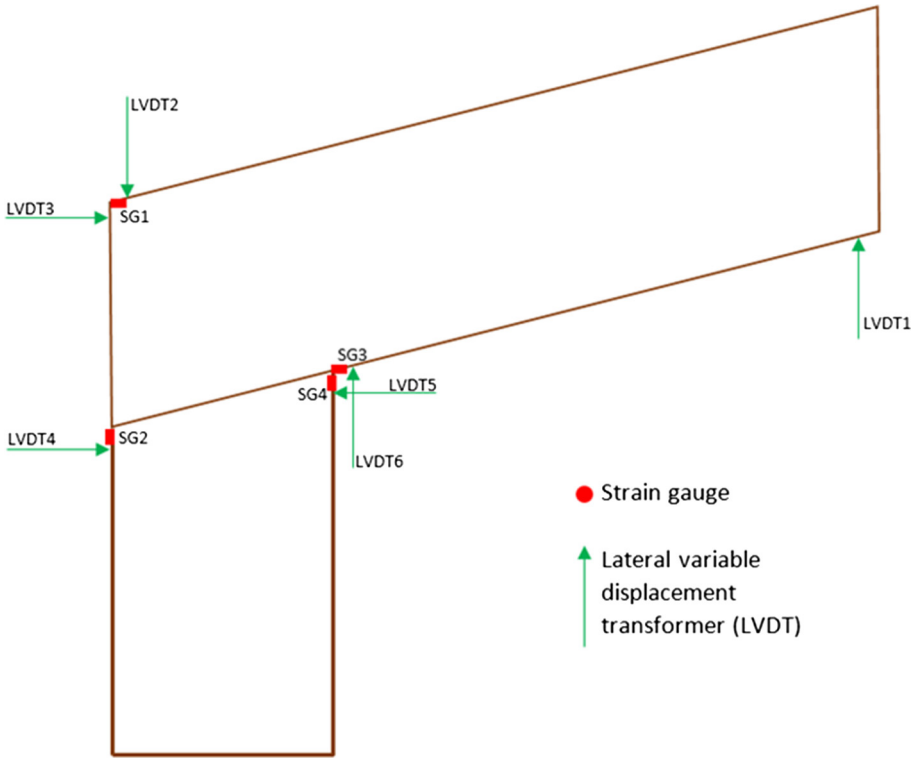

Fig. 7. Instrumentation on frame corner.

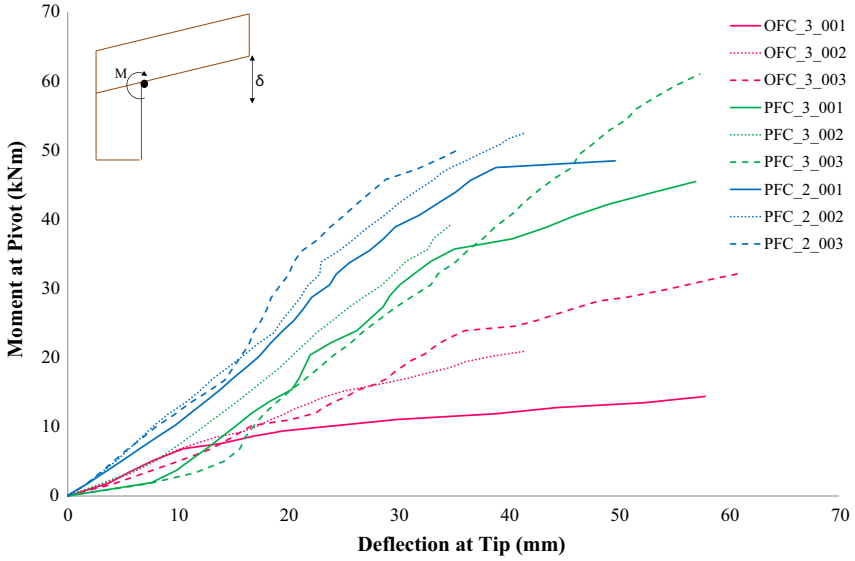

Fig. 8. Moment-deflection graphs of all specimens.

connection could be assessed without other factors influencing strength of the system.

4.3.2. Failure modes

The primary failure mode observed for each specimen set is detailed in Table 3. Failure was categorised into two primary failure modes; failure of the web material and failure of the moment connection. The box beams failure mode changed for the varying materials and bar configuration.

Failure of the web material was the primary failure mode observed in the specimens with OSB webs. Under an applied load of 10kN the panel shear stress was 0.84 N/mm^2. Thus the OSB material was not sufficiently strong enough to transfer loads between the flanges and into the post since the internal bond strength of the OSB was approximately 0.32 N/mm^2 [17]. Failure

Table 3
Failure modes observed for each set.

Set ID	Failure Mode
OFC_3	Web failure
PFC_3	Web failure and Connection failure
PFC_2	Connection failure

of the OSB web was characterised by popping sounds which were audible from early in the testing. This failure mode was not observed as frequently in the sets with plywood webs since the shear strength of the plywood is much greater than that of the OSB, approximately 1.86 N/mm^2 [18].

In specimens where failure occurred in the web material, crushing of the web material at the front of the post was also observed. This was a further indication that the box sections did not have the strength required to effectively transfer high loads through the system. Similar behaviour was observed in the PFC_3 series however it was evident that glued-in rods were more active in these specimens with the build-up of stresses around the connection resulting in some cracking of timber at the back of the post.

Failure of the moment connection was further categorised into two modes; pull-out of the rod from the post and a tension failure of the timber in the vicinity of the connection arising from a build-up of stresses around connection. Failure of the timber around the rods arose as a result of the build-up of stresses in that area, the connection remained the strongest component in the system again resulting in a failure of the timber. This timber failure is however different to failure of the web material, here loads are being transferred more effectively through the rod to post.

4.3.3. Ultimate strength

Table 4 details the ultimate strengths achieved by each specimen at the point of structural failure.

The highest strengths were achieved by specimens in the PFC_3 set however variation within this set was relatively high with a coefficient of variation of 0.23. Variation within specimens was lowest within the PFC_2 set with a coefficient of variation of 0.04. In these specimens the moment connection was performing most effectively, evidenced by failure of the connection rather than failure of the beam or post material. The deflection behaviour of this set was preferential also, as presented in the section above. Specimens with plywood webs performed on average 2.22 times better in terms of strength than those with OSB webs. There was however no significant difference in strength between those plywood specimens with two embedded rods and those with three rods, as seen in Table 4. Despite the similar failure strengths achieved the coefficients of variation highlight the larger variation between specimens with two and those with three embedded rods. This difference in variation may be attributed to the failure modes in specimens with 3 rods which had timber failures in the element. Such failures would be expected to have a larger range due to the variability of the timber itself. In the specimens with 2 rods they failed primarily in the pull out of the rod which is a more consistent failure mode.

Given the difference in failure mode between the specimen sets, the results suggest that strength of two embedded rods is approaching the overall strength of the box section, after which the beam or flange material is just as likely to fail as the moment connection. There may also be group effects at play when three rods are used thus decreasing the effectiveness of the additional rod. Such group effects have been studied by [19–21].

4.3.4. Strains

In all specimens, strain on both the internal and external face of the post was measured as well as on the top and underside of the beam at the connection end on the PFC_2 and PFC_3 specimens. Fig. 7 shows the location of these strain gauges. The purpose of gathering strain readings in these positions is to validate which parts of the specimen were under compression or in tension and to evaluate how well load was being transferred through the section. This would allow the location of the neutral axis to be determined and allow validation of the theoretical predictions.

As illustrated in Fig. 9 the external face of the post experienced low stress until approaching failure, reaching an average tensile stress of 0.86 N/mm^2 at failure, where in some cases the timber split and failure was as a result of the sudden loss of bond between the flange and web material.

Strain measurements taken on the top and underside of the beam showed that the top face of the beam experienced minimal stress throughout loading until the point of failure where a steep increase in strain was observed. The underside of the beam however was under increasing compressive stress. Stress increased in a linear way until failure when, similar to the top face of the beam, a step increase in strain was observed. This increase was indicative of the brittle type failure observed.

A low tensile strain was observed at the outer face of the post. This was evidence of the effective load distribution over a larger region of timber due to the presence of the GiR. Conversely the absence of a GiR at the internal face of the post has resulted in higher compressive strain on the contact surface of the timber.

4.4. Comparison of theory and experimental findings

Using the method outlined in Section 3 it was predicted that the plywood box-section frame corner with two embedded rods (PFC_2) would fail in the connection when the applied moment reaches 43.1 kNm. From the experimental results presented in the previous section it can be seen that all specimens with two GiR surpassed this moment capacity (average failure moment 51.2 kNm) with 15.8% difference between predicted observed behaviour. The predicted behaviour makes use of Eq. (1) from the German National Annex to Eurocode 5 (DIN 1052:2008) [12]. However as Fig. 1 shows this equation provides and underestimation of pull out strength, which we believe is the key factor resulting in the variation between the prediction and observed results. For test specimens in which the failure did not occur in the GiR the theory is not relevant. With the addition of more GiR failure the failure mode would need to be managed to ensure it occurs in the GiR given the design method used. However it should be noted that when using additional rods the spacing between rods must be carefully considered so as to avoid certain group effects that may

Table 4
Summary of strengths reached at structural failure.

Set ID	Ultimate Applied Load (kN)	Moment at Pivot (kNm)	Coefficient of Variation	Failure Mode
OFC_3_001	10.1	17.1	0.27	OSB web
OFC_3_002	12.4	21.0		OSB web
OFC_3_003	19.0	32.1		OSB web
PFC_3_001	28.1	47.6	0.23	Ply web and tension failure
PFC_3_002	24.0	40.6		Tension failure
PFC_3_003	41.0	69.3		Tension failure
PFC_2_001	28.7	48.5	0.04	Rod pull-out
PFC_2_002	31.0	52.5		Rod pull-out
PFC_2_003	31.1	52.5		Tension failure around rod

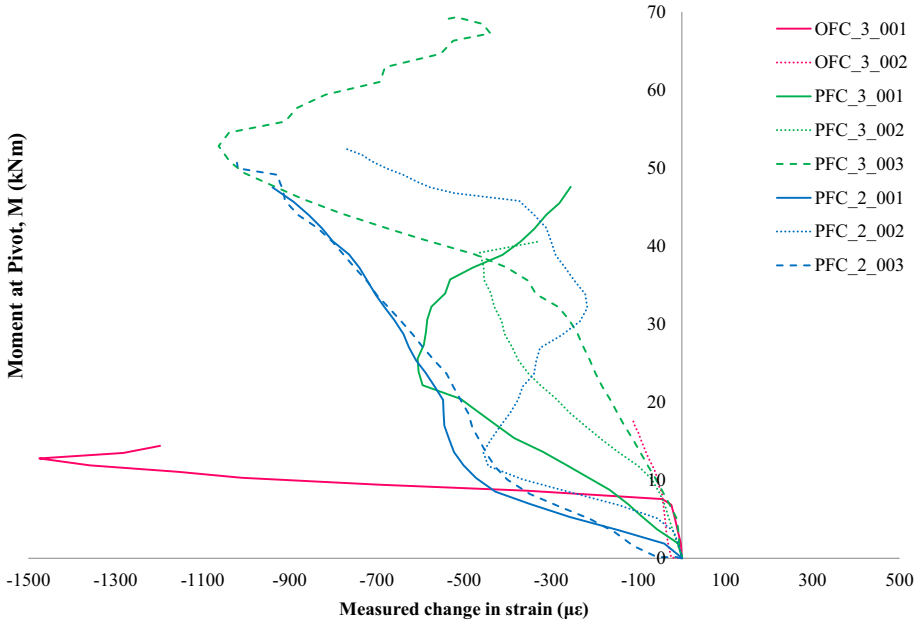

Fig. 9. Strain recorded with increasing load on external face of post on each specimen.

lead to a reduction in the overall strength of the system [19,21]. It should also be noted that where steel rods are being used the system is designed such that failure is ductile thus allowing for an even distribution of forces among all rods and avoiding the premature failure due to group effects.

5. Conclusions

This research has demonstrated that glued-in basalt FRP rods have good potential for use as moment connections in portal frame structures. The key findings of the research are:

- Additional rods do not appear to have a significant impact upon the overall strength of the frame corner. Further experimental work would be required to investigate this influence of group effects and determination of optimum spacing for multiple rods.
- The addition of another rod did increase the variability within specimens, by up to 6 times. It is therefore recommended that the number of rods used is assessed before specification and their spacing considered so as to negate any group effects and to realise the full benefit of additional rods. If there is insufficient spacing available for the number of rods required it is suggested that other methods of strengthening the connection are considered, e.g. using larger diameter rods, increasing embedded length of the rod or by increasing the glueline thickness or that steel rods are used and the system designed for ductile failure.
- Due to limitations on size in the testing apparatus the study considered only frame corners with a 5° pitch. Further testing with steeper pitch is recommended, 10°/15° more common roof pitch.
- Larger scale testing would be beneficial where the post is not as short so as to evaluate any movement or any restrictions that were imposed in this test series by holding the specimen post so close to the embedded rods.
- The theoretical stress profile derived from first principles provides a prediction for the strength of the connection that is on average accurate to within 15.8%.

Acknowledgement

This research was funded by the Department of Agriculture, Food and the Marine of the Republic of Ireland under the FIRM/RSF/COFORD scheme as part of 'Innovation in Irish Timber Usage' (project ref. 11/C/207).

References

[1] D. Smedley, P. Alam, M. Ansell, George Street, St. Albans, UK–a case study in the repair of historic timber structures using bonded-in pultruded plates, . . . of 9th World Conference on Timber . . ., no. 2006, 2006.
[2] P. Alam, M.P. Ansell, D. Smedley, Mechanical repair of timber beams fractured in flexure using bonded-in reinforcements, Compos. B Eng. 40 (2) (2009) 95–106.
[3] E. Gehri, High performing jointing technique using glued-in rods, in: 11th World Conference on Timber Engineering 2010, WCTE 2010, 2010.
[4] R. Bainbridge, C. Mettem, K. Harvey, M. Ansell, Bonded-in rod connections for timber structures—development of design methods and test observations, Int. J. Adhes. Adhes. 22 (1) (2002) 47–59.
[5] J.G. Broughton, A.R. Hutchinson, LICONS Task 2-Sub tast 2.2, 2004.
[6] D. Yeboah, Rigid Connections in Structural Timber Assemblies, Queen's University Belfast, 2012.
[7] C. O'Neill, D. McPolin, S.E. Taylor, A.M. Harte, Basalt fibre reinforced polymer rods for glued connections in low grade timber, Adv. Compos. Constr., ACIC (2015).
[8] EN 338, Structural Timber – Strength Classes, European Committee for Standardisations, Brussels, Belgium, 2009.
[9] EN 408, Timber Structures – Structural Timber and Glued Laminated Timber – Determination of Some Physical and Mechanical Properties, European Committee for Standardisations, Brussels, Belgium, 2012.
[10] Magmatech, RockBar Corrosion resistant basalt fibre reinforcing bars, 2013. Technical information leaflet. [Online]. Available: http://magmatech.co.uk/downloads/ROCKBAR_4P.pdf.
[11] Rotafix Ltd, Rotafix Structural Adhesive (LM) – Epoxy Bonding Adhesive, 2015.
[12] Deutsches Institut für Normung e.V, DIN 1052. Entwurf, Berechnung und Bemessung von Holzbauwerken – Allgemeine Bemessungsregeln und Bemessungsregeln für den Hochbau. Berlin, Germany, 2008.
[13] J. Brady, A. Harte, Flexural reinforcement of glue-laminated timber beams using prestressed FRP plates, in: 4th International Conference of Advanced Composites in Construction (ACIC), 2008.
[14] A.H. Buchanan, Bending strength of lumber, ASCE J. Struct. Eng. 116 (5) (1990) 1213–1229.
[15] G. Patrick, The Structural Performance of FRP Reinforcedglue Laminated Beams Made From Homegrown Sitka Spruce, Queen's University Belfast, 2004.
[16] EN 1995-1-1, Eurocode 5: Design of Timber Structures – Part 1-1: General – Common Rules and Rules for Buildings, European Committee for Standardisations, Brussels, Belgium, 2008.

[17] Coillte Panel Products, SmartPly OSB3 Data Sheet, 2013.
[18] AS Latvijas Finieris, Plywood Handbook, 2010.
[19] G. Parida, H. Johnsson, M. Fragiacomo, Provisions for ductile behavior of timber-to steel connections with multiple glued-in rods, J. Struct. Eng. 139 (9) (2013) 1468–1477.
[20] E. Gonzalez, C. Avez, T. Tannert, Timber joints with multiple glued-in steel rods, J. Adhesion 92 (7–9) (Sep. 2016) 635–651.
[21] E. Gehri, Ductile behaviour and group effect of glued-in steel rods, in: International RILEM Symposium on Joints in Timber Structures, RILEM Publications s.a.r.l., Stuttgart, Germany, 2001, pp. 333–342.